Glycobiology, 2020, vol. 30, no. 10, 817–829
doi: 10.1093/glycob/cwaa024
Advance Access Publication Date: 9 March 2020
Original Article

OXFORD

Genetic Disorders of Glycosylation

HNK-1 sulfotransferase modulates α-dystroglycan glycosylation by 3-O-sulfation of glucuronic acid on matriglycan

M Osman Sheikh[2], David Venzke[4], Mary E Anderson[4], Takako Yoshida-Moriguchi[4], John N Glushka[2], Alison V Nairn[2], Melina Galizzi[2], Kelley W Moremen[2,3], Kevin P Campbell[4,1] and Lance Wells[1,2,3]

[2]Complex Carbohydrate Research Center, and [3]Department of Biochemistry and Molecular Biology, University of Georgia, Athens, GA 30602, USA, and [4]Department of Molecular Physiology and Biophysics, Department of Neurology, Howard Hughes Medical Institute, University of Iowa Roy J. and Lucille A. Carver College of Medicine, Iowa City, IA 52242, USA

[1]To whom correspondence should be addressed: Tel: +1-319-335-7867; Fax: +1-319-335-6957; e-mail: kevin-campbell@uiowa.edu and Tel: +1-706-542-7806; Fax: +1-706-542-4412; e-mail: lwells@ccrc.uga.edu

Received 14 July 2019; Revised 26 February 2020; Accepted 26 February 2020

Abstract

Mutations in multiple genes required for proper O-mannosylation of α-dystroglycan are causal for congenital/limb-girdle muscular dystrophies and abnormal brain development in mammals. Previously, we and others further elucidated the functional *O*-mannose glycan structure that is terminated by matriglycan, [(-GlcA-β3-Xyl-α3-)$_n$]. This repeating disaccharide serves as a receptor for proteins in the extracellular matrix. Here, we demonstrate in vitro that HNK-1 sulfotransferase (HNK-1ST/carbohydrate sulfotransferase) sulfates terminal glucuronyl residues of matriglycan at the 3-hydroxyl and prevents further matriglycan polymerization by the LARGE1 glycosyltransferase. While α-dystroglycan isolated from mouse heart and kidney is susceptible to exoglycosidase digestion of matriglycan, the functional, lower molecular weight α-dystroglycan detected in brain, where HNK-1ST expression is elevated, is resistant. Removal of the sulfate cap by a sulfatase facilitated dual-glycosidase digestion. Our data strongly support a tissue specific mechanism in which HNK-1ST regulates polymer length by competing with LARGE for the 3-position on the nonreducing GlcA of matriglycan.

Key words: α-dystroglycan, congenital muscular dystrophy, glycosylation, O-mannosylation, sulfotransferase

Introduction

It has been recently appreciated that proper glycosylation of the cell surface glycoprotein α-dystroglycan (α-DG) is required, as part of the dystrophin–glycoprotein complex, for linking the actin cytoskeleton to components of the extracellular matrix (ECM) in muscle and brain tissue (Wells 2013; Yoshida-Moriguchi and Campbell 2015; Manya and Endo 2017; Sheikh et al. 2017; Hohenester 2018; Kanagawa and Toda 2018). Disease subtypes of congenital muscular dystrophy (CMD) that result in hypoglycosylated α-DG are referred to as secondary or tertiary dystroglycanopathies (Brockington et al. 2010; Beedle et al. 2012; Roscioli et al. 2012; Willer et al. 2012; Riemersma et al. 2015). Thus, a comprehensive understanding of the composition, biosynthesis and regulation of the α-DG functional glycan is essential for identifying and studying the biochemical etiologies of various dystroglycanopathies. Our groups, along with others (Gerin et al. 2016; Kanagawa et al. 2016), have recently

contributed to this by identifying a novel phospho-ribitol component and the primer region of the functionally relevant *O*-mannosyl-initiated α-DG glycan (Praissman and Wells 2014; Willer et al. 2014; Praissman et al. 2016). The phospho-ribitol moieties, recently identified in humans, contribute to bridging a phosphorylated trisaccharide on α-DG to a glycosaminoglycan (GAG)-like polymer, matriglycan [(-GlcA-β3-Xyl-α3-)$_n$] that binds to certain proteins in the ECM (Figure 1A). A culmination of work from multiple groups has since proposed this functionally relevant Core M3 *O*-mannose structure on α-DG to be (-GlcA-β3-Xyl-α3-)$_n$-GlcA-β4-Xyl-β2-ribitol-1-P-ribitol-1-P-3-GalNAc-β3-GlcNAc-β4-(6-P)-Man-O-(Ser/Thr) (Yoshida-Moriguchi et al. 2010; Inamori et al. 2012; Inamori et al. 2013; Yoshida-Moriguchi et al. 2013; Praissman et al. 2014; Willer et al. 2014; Gerin et al. 2016; Kanagawa et al. 2016; Manya et al. 2016; Praissman et al. 2016; Sheikh et al. 2017).

Matriglycan (Yoshida-Moriguchi and Campbell 2015) is the laminin globular (LG)-domain binding epitope synthesized by the Golgi-resident bifunctional glycosyltransferase LARGE1 or its paralog LARGE2 (Inamori et al. 2012; Inamori et al. 2013). To date, a precise understanding of how matriglycan chain lengths are directly modulated is not entirely known. However, overexpression of LARGE1 or LARGE2 in cells increases the functional glycosylation and apparent molecular weight of α-DG (Barresi et al. 2004; Patnaik and Stanley 2005; Nakagawa et al. 2012, 2013) and α-DG isolated from various tissues has vastly different and apparent molecular weights (Kunz et al. 2005; Yoshida-Moriguchi and Campbell 2015) (Figure 1B). Conversely, the sulfation of the α-DG functional glycan by the human natural killer-1 sulfotransferase (HNK-1ST/carbohydrate sulfotransferase [CHST10]) has been suggested to play a role in inhibiting extension (Nakagawa et al. 2012, 2013). The Golgi resident HNK-1ST is best known for its involvement in synthesizing the canonical HNK-1 carbohydrate epitope (SO_3-3-GlcA-β3-Gal-β4-GlcNAc-R) on N-linked glycans. HNK-1ST catalyzes the transfer of a sulfo group from 3′-phosphoadenosine 5′-phosphosulfate (PAPS) to carbon-3 of nonreducing end, terminal glucuronic acid that is β3-linked to *N*-acetyllactosamine (LacNAc) on glycoprotein targets in the brain, such as neural cell adhesion molecule (NCAM), myelin-associated glycoprotein (MAG), tenascin-R and tenascin-C (McGarry et al. 1983; Kruse et al. 1984; Chou et al. 1986; Xiao et al. 1997; Ong et al. 2002; Yagi et al. 2010; Morise et al. 2017). In addition to these well-studied cell adhesion and ECM-binding target molecules, HNK-1ST is capable of generating the HNK-1 epitope on glycolipids (Chou et al. 1986), sulfating *O*-glycan structures on proteoglycans (Hashiguchi et al. 2011), as well as sulfating estrogen and other glucuronidated steroid hormones contributing to hormone regulation and fertility (Suzuki-Anekoji et al. 2013).

Notably, the canonical HNK-1 epitope that is β2-linked to O-linked mannose (Core M1 and M2-type) was detected on glycopeptides isolated from rabbit brain (Yuen et al. 1997), and more specifically, detected on *O*-mannose glycans derived from phosphacan, a secreted chondroitin sulfate proteoglycan in the brain (Morise et al. 2014; Dwyer et al. 2015). Interestingly, before complete elucidation of the functionally relevant Core M3 structure, it was previously demonstrated that HNK-1ST sulfates an unknown glycan structure on α-DG that is sensitive to treatment with hydrofluoric acid (Nakagawa et al. 2013), thus presumably after a phosphodiester-linked glycan moiety. Since the LARGE glycosyltransferases possess both xylosyltransferase and glucuronyltransferase activities, it was hypothesized that HNK-1ST may sulfate glucuronic acid (GlcA) residues synthesized by LARGE1 or LARGE2, which has yet to be directly validated (Yoshida-Moriguchi and Campbell 2015).

In this report, we extend our studies of the functional glycan by directly investigating HNK-1ST sulfotransferase activity on LARGE-dependent matriglycan polymerization using purified components, while also probing the tissue-dependent susceptibility of α-DG to exoglycosidase digestion. Our studies demonstrate that HNK-1ST catalyzes 3-O-sulfation of terminal GlcA on matriglycan and prevents further matriglycan extension by LARGE1. Furthermore, exoglycosidase digestion analyses of matriglycan derived from α-DG isolated from various tissues reveals that sulfated α-DG from brain, where HNK-1ST expression is high, is amenable to digestion only upon removal of the sulfate cap by pretreatment using a sulfatase. These results strongly support a tissue specific mechanism in which HNK-1ST and LARGE compete to define the length of matriglycan on α-DG.

Results and discussion

Exoglycosidase digestion of matriglycan from different tissues

Using a recently developed dual exoglycosidase digestion assay (Briggs et al. 2016), we sought to probe the glycosylation status of native α-DG isolated from different mouse tissues. Wheat germ agglutinin (WGA)-enriched extracts from mouse brain, heart and kidney were treated with a β-glucuronidase (bGus) and an α-xylosidase (XylS) simultaneously (Moracci et al. 2000; Salleh et al. 2006) to degrade matriglycan extensions. Western blot analysis of the digestion products using an anti-α-DG-core antibody demonstrates that α-DG from mouse heart and kidney are susceptible to bGus/XylS digestion of matriglycan (Figure 1B). Furthermore, the digestion of heart and kidney α-DG that results in loss of binding to the ECM ligand laminin in an overlay assay (Figure 1C). However, dual-glycosidase treatment of α-DG from brain fails to affect molecular weight or laminin binding (Figure 1), suggesting a possible cap on matriglycan.

HNK-1ST transfers a sulfo group to GlcA-β4-Xyl-β-pNP and prevents extension by LARGE1

Since HNK-1ST (gene symbol CHST10) has been implicated in sulfating a glycan structure on α-DG, we decided to test HNK-1ST's sulfotransferase activity directly in an isolated system. To validate HNK-1ST's capability to modify noncanonical HNK-1 epitopes, we synthesized GlcA-β4-Xyl-β-pNP as a putative acceptor substrate using a recombinant secreted form of the β-1,4-glucuronyltransferase B4GAT1 (Praissman et al. 2014) to transfer GlcA to Xyl-β-*para*-nitrophenyl. This resultant disaccharide, linked to pNP at the reducing terminus, was selected since it is the primer for LARGE1-dependent matriglycan synthesis (Praissman et al. 2014; Willer et al. 2014). As the enzyme source, a secreted form of HNK-1ST, also lacking its transmembrane region, was expressed and purified from HEK293F cells. In a reaction containing PAPS as a sulfo-donor, HNK-1ST catalyzed the transfer of a sulfo group from PAPS to GlcA-β4-Xyl-β-pNP, as detected by ion trap mass spectrometry (ITMS) in negative ion mode (Figure 2A and B). MS^n analyses of the reaction product (*m/z* 526) confirm the structure, SO_3-GlcA-β4-Xyl-β-pNP (Figure 2D). In an attempt to use Xyl-β-pNP as an acceptor, HNK-1ST was unable to generate any detectable sulfated Xyl species (data not shown).

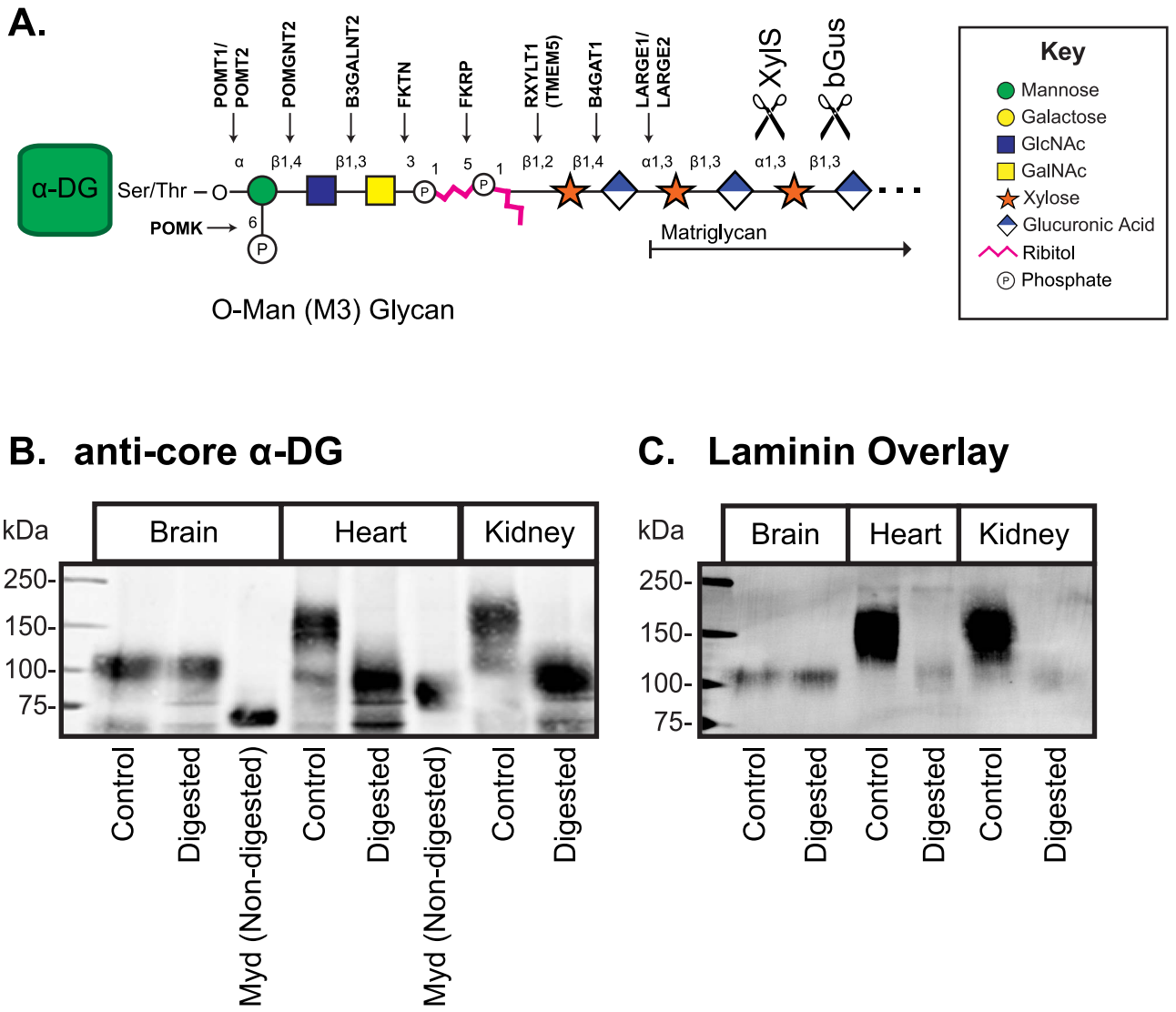

Fig. 1. Exoglycosidase digestion of matriglycan from different tissues. (A) Fully elaborated M3 glycan showing susceptible sites for exoglycosidase digestion. Glycan symbols and substituents are adapted from the Symbol Nomenclature for Glycans (Varki et al. 2015) and (Sheikh et al. 2017). (B) WGA-enriched extracts from mouse brain, heart and kidney were treated with a β-glucuronidase (bGus) and an α-xylosidase (XylS) simultaneously, followed by immunoblot analysis using an anti-α-DG-core antibody (AF6868). (C) A laminin overlay assay was performed by incubating membranes with Natural Mouse Laminin from Engelbreth-Holm-Swarm (EHS) sarcoma. Myd: The Myodystrophy (Myd) mouse model (Large1$^{myd/myd}$) possesses a mutation in the *LARGE1* gene, resulting in hypoglycosylated α-DG, and is used as a nondigested negative control (Grewal et al. 2001). The images shown are the representative images of $N = 3$. This figure is available in black and white in print and in color at *Glycobiology* online.

To determine if LARGE1 can synthesize matriglycan on a structure terminating in sulfated GlcA, we took the reaction mixture from Figure 2B, which contained both the sulfated disaccharide and unreacted GlcA-β4-Xyl-β-pNP, and performed a subsequent reaction with LARGE1 in the presence of UDP-GlcA and UDP-Xyl as the sugar-donor molecules. Remarkably, LARGE1 had the ability to extend GlcA-β4-Xyl-β-pNP (*m/z* 446) to a higher order polymer (*m/z* 754, GlcA-β3-Xyl-α3-GlcA-β4-Xyl-β-pNP and presumably even higher order polymers that were undetected) (Figure 2C), while SO_3-GlcA-β4-Xyl-β-pNP remained unmodified as determined by the increase in its relative abundance with respect to the *m/z* 446 peak (Figure 2B vs. C). No branched, sulfated structures were detected, consistent with previous reports were consistent that LARGE1 does not possess branching activity (Praissman et al. 2014).

HNK-1ST transfers a sulfo group to nonreducing end GlcA of matriglycan and prevents extension by LARGE1

Additionally, we performed a similar assay using a mixture of matriglycan polymers of varying lengths generated by LARGE1 (Figure 3). As anticipated, HNK-1ST was capable of sulfating any matriglycan structure terminating in GlcA at the nonreducing end (note the reaction product ions at *m/z* 526, 834 and 1142; Figure 3B, Supplementary Figure S1). These results are consistent with previous reports of HNK-1ST having the ability to modify synthetic acceptor substrates terminating in β-GlcA in vitro (Bakker et al. 1997). MS2 fragmentation of these structures revealed only terminal GlcA sulfation, as no internal GlcA sulfation fragments (data not shown), or species terminating in sulfated Xyl in the MS1

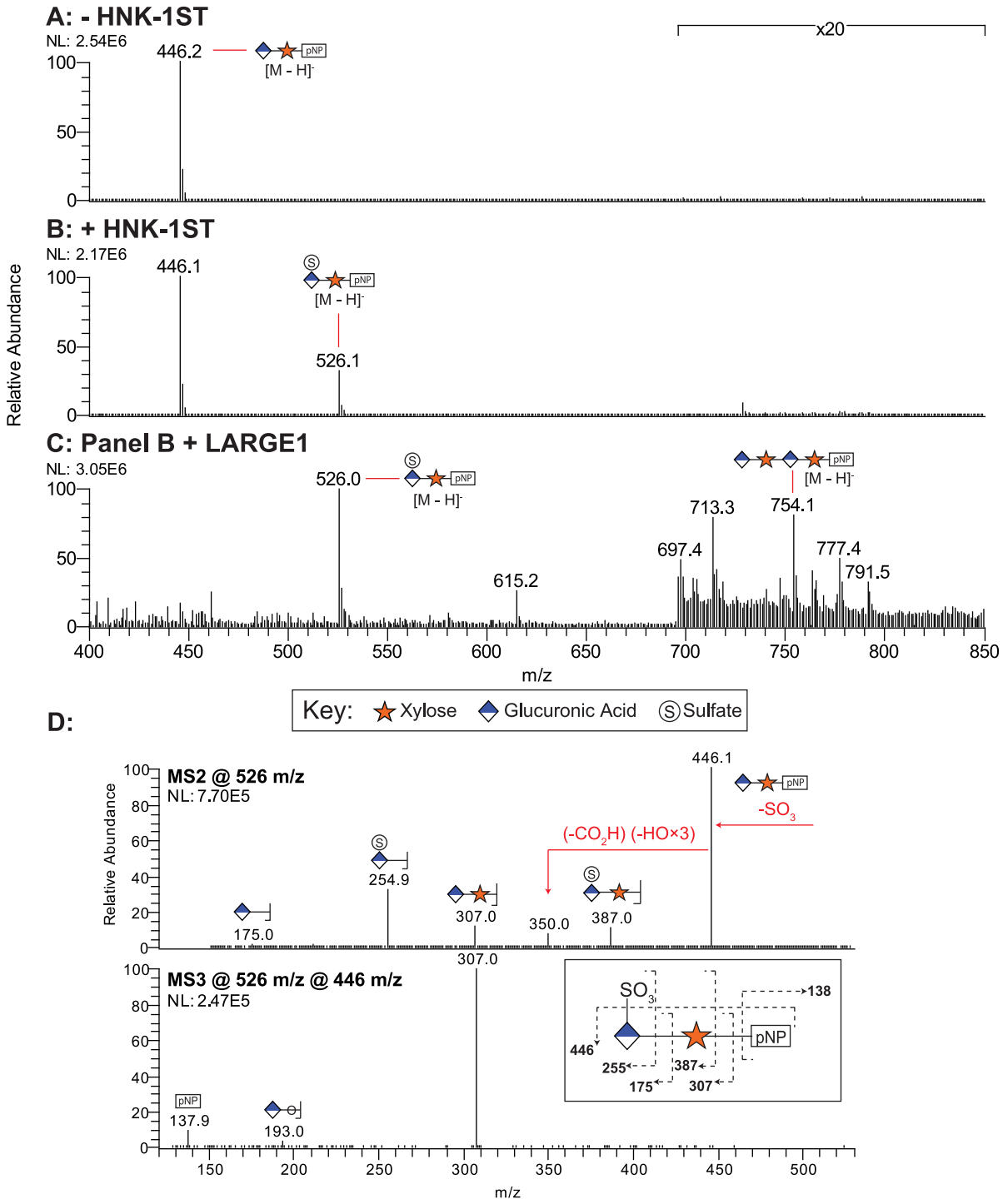

Fig. 2. HNK-1ST transfers a sulfo group to GlcA-β4-Xyl-β-pNP and prevents extension by LARGE1. GlcA-β4-Xyl-β-pNP acceptor substrate was incubated without (A) or with (B) HNK-1ST and PAPS donor, and the reaction was analyzed by ion trap mass spectrometry (ITMS) in negative ion mode. Annotated peaks were confirmed by MS/MS. (C) Reaction from Panel B was further incubated with UDP-GlcA and UDP-Xyl with LARGE1. (D) MS^n analysis of the HNK-1ST product confirms the sulfate being located on GlcA. Spectra shown are the representative of $N = 3$. This figure is available in black and white in print and in color at *Glycobiology* online.

could be detected. As demonstrated with sulfo-GlcA-β4-Xyl-β-pNP, while LARGE1 was capable of extending matriglycan structures terminating in Xyl or nonsulfated GlcA (*m/z* 446, 578 and 886), LARGE1 was unable to extend structures sulfated by HNK-1ST (*m/z* 526, 834 and 1142), as judged by their presence and increase in relative abundances after the LARGE1 reaction (Figure 3C). A summary of the expected and observed glycoforms are listed in Table I. Taken together, these results demonstrate direct inhibition of LARGE1-mediated matriglycan polymerization due to sulfation by HNK-1ST.

Table I. Calculated matriglycan polymers. Species shaded in gray were observed in this study

		Calculated mass (Da)	$[M–H]^-$ (m/z)	+Sulfate (+80) (m/z)
Repeats	Starting GlcA-β4-Xyl-β-pNP mass →	447	446	526
1	+Xyl (+132)	579	578	658
	+GlcA (+176)	755	754	834
2	+Xyl (+132)	887	886	966
	+GlcA (+176)	1063	1062	1142

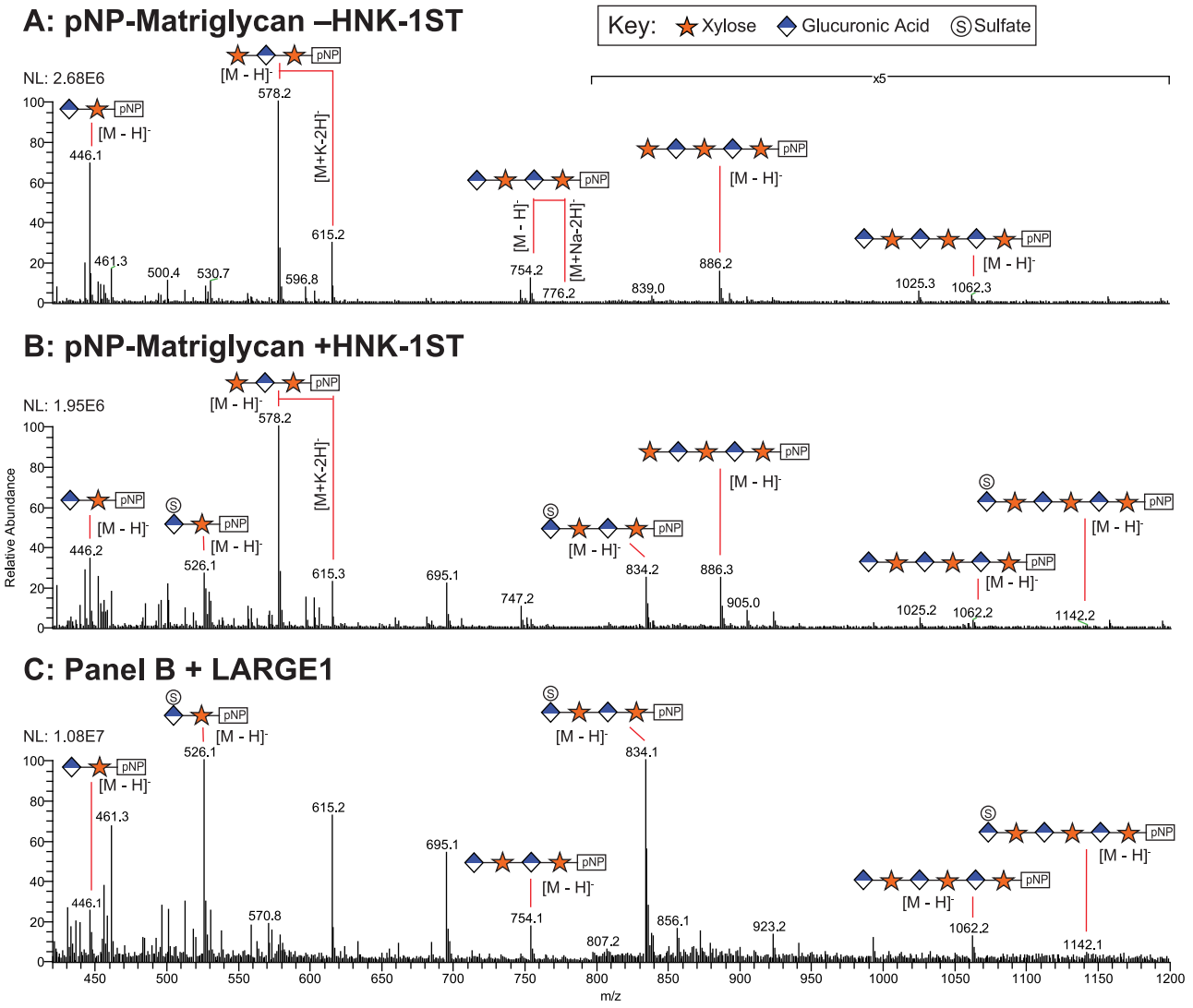

Fig. 3. HNK-1ST transfers a sulfo group to nonreducing end GlcA of matriglycan and prevents extension by LARGE1. pNP-matriglycan (heterogeneous mixture) acceptor substrate was incubated without (A) or with (B) HNK-1ST and PAPS donor, and the reaction was analyzed by ITMS in negative ion mode. Annotated peaks were confirmed by MS/MS. (C) Reaction from Panel B was further incubated with UDP-GlcA and UDP-Xyl with LARGE1. Spectra shown are the representative of $N = 3$. This figure is available in black and white in print and in color at *Glycobiology* online.

Nuclear magnetic resonance analysis of HNK-1ST reaction product demonstrates sulfation at position 3 of GlcA

As mentioned previously, the classical HNK-1 structure terminates in a sulfo group that is 3-*O*-linked to GlcA attached to LacNAc. To determine if the sulfation position of GlcA on matriglycan catalyzed by HNK-1ST is as generated on the classical HNK-1 structure, we analyzed the HNK-1ST reaction product, SO_3-GlcA-β4-Xyl-β-pNP by nuclear magnetic resonance (NMR). The one-dimensional ^{1}H-NMR spectrum of unmodified GlcA-β4-Xyl-β-pNP revealed the presence (~4-fold excess) of Xyl-β-pNP starting material, presumably from an incomplete B4GAT1 reaction since the reaction product was not purified away from Xyl-β-pNP starting material (Figure 4A). Comparison of the untreated and sulfated 1D proton and COSY

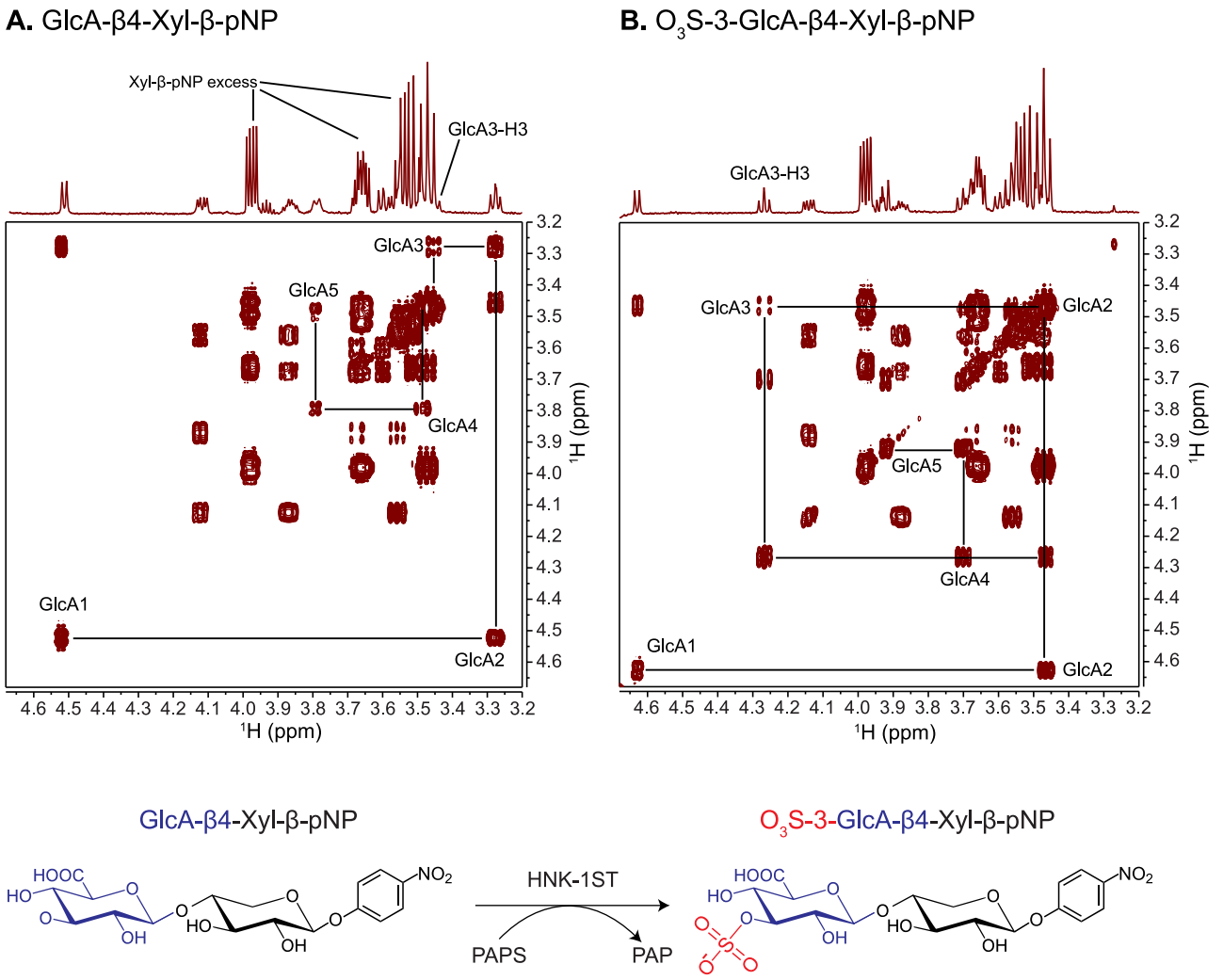

Fig. 4. Nuclear magnetic resonance (NMR) analysis of HNK-1ST reaction product demonstrates sulfation at position 3 of GlcA. (A) GlcA-β4-Xyl-β-pNP starting material was analyzed by COSY ^{1}H-^{1}H-NMR and compared to the HNK-1ST-sulfated reaction product (B). This figure is available in black and white in print and in color at *Glycobiology* online.

spectra clearly indicate the downfield GlcA-H3 shift due to the sulfate on the 3′hydroxyl group, defining the complete linkage as SO_3-3-GlcA-β4-Xyl-β-pNP (Figure 4, Table II). Thus, HNK-1ST is capable of sulfating matriglycan, a noncanonical substrate, at the 3-position of GlcA, in vitro, which is the same position that LARGE adds a nonreducing Xyl residue to during extension.

Sulfation serves as a cap on matriglycan

Since α-DG isolated from mouse brain was resistant to dual glycosidase treatment, we speculated that terminal GlcA sulfation may be inhibiting the glucuronidase activity of bGus, thus blocking subsequent digestion by XylS (Figure 1). To test the effect of sulfation on bGus activity, we digested unsulfated and sulfated GlcA-β4-Xyl-β-pNP with bGus and detected the reaction products by ITMS (Figure 5A). Unsulfated GlcA-β4-Xyl-β-pNP (*m/z* 446) was efficiently digested as determined by the disappearance of the *m/z* 446 peak and the increase in relative abundance of the Xyl-β-pNP (*m/z* 316) peak. However, in a parallel reaction, sulfo-GlcA-β4-Xyl-β-pNP (*m/z* 526) was resistant to bGus digestion.

Next, we attempted to remove the suspected sulfate cap on native brain α-DG by use of a commercially available arylsulfatase in conjunction with the dual glycosidase assay used above. This was followed by western blot analysis using the antiglyco-α-DG antibody (IIH6) that recognizes matriglycan (Figure 5B) (Ervasti and Campbell 1993; Yoshida-Moriguchi and Campbell 2015). Sulfatase treatment facilitated the digestion of matriglycan on brain α-DG, owing to the time-dependent reduction of the IIH6 signal (Figure 5B). Sulfatase treatment was not required for the exoglycosidase digestion of matriglycan on skeletal muscle α-DG (Figure 5C). Additionally, the observed band shifts were not caused by sulfatase treatment alone (Supplementary Figure S2). Taken together, sulfated GlcA is resistant to bGus digestion and removal of the sulfate cap facilitates dual glycosidase digestion of brain α-DG.

Transcript abundance of HNK-1ST is greatest in the brain

To further explore why the capping seemed to be prevalent in α-DG isolated from brain, we analyzed the transcripts of major genes

Table II. Summary of observed and literature GlcA/Xyl NMR chemical shifts

	GlcA-Xyl-pNP[a]		SO_3-3-GlcA-Xyl-pNP[a]		Inamori et al.[b]		Voshol et al.[c]
Residue	GlcA	Xyl	SO_3-3-GlcA-	Xyl	GlcA	Xyl	SO_3-3-GlcA-
1	4.52	5.18	4.63	5.19	4.72	5.38	4.77
2	3.27	3.60	3.47	3.60	3.38	3.74	
3	3.45	3.67	4.27	3.68	3.54	3.88	4.33
4	3.48	3.87	3.70	3.88	3.51	3.70	
5	3.79	3.55, 4.12	3.93	3.56, 4.14	3.75	3.69, 3.95	

[a](SO_3-3) ± GlcA-β1,4-Xyl-β-pNP chemical shifts referenced to residual HDO at 4.7 ppm.
[b]Inamori et al. (2012), for terminal disaccharide in GlcA-β1,3-Xyl-α1,3-GlcA-MU, where MU = 4-methylumbelliferyl.
[c]Voshol et al. (1996), SO_4-3-GlcA-β1,3-Gal-β1,4-GlcNAc, taken at different temperature.

involved with the synthesis of the functional Core M3 structure in the various mouse tissues used in this study (Figure 6). While there is some variability in the expression profiles of the selected genes across the different tissues, a striking difference is revealed among the analysis of *LARGE1*, *LARGE2* and *HNK-1ST* (Figure 6A). As demonstrated previously, *LARGE1* is expressed in all tissues analyzed, with greater expression in heart and brain, whereas *LARGE2* is preferentially expressed in kidney (Peyrard et al. 1999; Grewal et al. 2005). The relative transcript abundance of *HNK-1ST* is greatest in the brain, and comparisons of *HNK-1ST* expression relative to either *LARGE2* or *LARGE1* reveal a 5- to 10-fold increase in expression in brain, respectively (Figure 6B) (Kleene and Schachner 2004; Kizuka and Oka 2012). These results are consistent with our observation that brain α-DG is of smaller molecular weight and capped with sulfate to a greater degree than in other analyzed tissues.

Conclusion

In summary, we demonstrated that HNK-1ST possesses in vitro activity toward nonreducing end GlcA-terminated matriglycan and that sulfation of GlcA blocks LARGE-mediated matriglycan extension. Sulfation of matriglycan by HNK-1ST is at the 3-position of GlcA, the same site of αXyl linkage. Thus, the mechanism by which sulfation of GlcA inhibits LARGE-mediated matriglycan extension is by a sulfate group occupying the site for Xyl attachment (Figure 6C). Reminiscent of our model, HNK-1ST sulfation of terminal GlcA in a GAG-linkage tetrasaccharide has also been demonstrated to inhibit chondroitin sulfate synthesis on the proteoglycan thrombomodulin (Hashiguchi et al. 2011; Nakagawa et al. 2011). Outstanding questions include the significance of matriglycan chain length and sulfation on recruitment of specific binding partners as well as any avidity enhancements longer chains may induce due to multivalent interactions. While it is appreciated that longer matriglycan polymers may assist in the structural cohesion of muscle and heart tissue, the function of shorter, sulfated matriglycan in the brain, where HNK-1ST expression is the highest, is unclear. Of the five carboxy-terminal LG-domains in laminin-α chains residing in the ECM, matriglycan interactions have been mapped to the LG4/5 domains (Talts et al. 1999; Tisi et al. 2000; Smirnov et al. 2002; Briggs et al. 2016), whereas direct interactions with the classical HNK-1 epitope occur in the LG2 domain (Hall et al. 1993; Hall et al. 1997; Bhunia et al. 2010). Interestingly, while both skeletal muscle and brain α-DG bind laminin-1, -2 and -8 isoforms, brain α-DG preferentially binds to Laminin 511/521 (previously referred to as Laminin-10/11) (Aumailley et al. 2005; McDearmon et al. 2006). Whether this preferential binding is regulated in part by matriglycan sulfation remains to be investigated. Targeted, HNK-1ST-mediated GlcA sulfation of matriglycan may constitute an additional, yet poorly understood, mechanism of regulating α-DG's glycans binding to ECM components.

Materials and methods

Protein expression and purification

The *Thermotoga maritima* bGus was expressed and purified as previously described (Salleh et al. 2006; Briggs et al. 2016). The enzyme's bGus activity was determined by the hydrolysis of pNP-β-D-GlcA in 100 µL reactions containing various amounts of bGus in 100 mM NaOAc pH 5.5 at 65°C for 30 min. Assays were quenched by the addition of 100 µL of 50 mM NaOH, and the release of pNP was determined spectrophotometrically by measuring absorbance at 405 nm (A_{405}).

An amino-terminal His_6-tagged version of the *Sulfolobus solfataricus* XylS was generated as follows. The full-length coding region for XylS was amplified from pT7SCII-XylS (Kind gift from Dr. Marco Moracci, University of Naples Federico II) (Moracci et al. 2000) by polymerase chain reaction (PCR) using the following primers (start codon indicated in bold and stop codon (reverse complement) underlined):

XylS-Donor-Forward: 5′-GGGGACAAGTTTGTACAAAAAAGCAGGCTTC**ATG**AGAATAGGGAATTTAAATG and XylS-Donor-Reverse: 5′- GGGGACCACTTTGTACAAGAAAGCTGGGTTCTAACCC. The resultant XylS PCR fragment was cloned into pDONR221 (Invitrogen, Carlsbad, CA) using a Gateway BP Clonase II reaction to generate the entry vector, pDONR221-XylS, which was subsequently cloned into the pDEST17 destination vector (Invitrogen, Carlsbad, CA) using a Gateway LR Clonase II reaction to generate the final vector, pDEST17-HisXylS, which was verified by restriction digest analysis and DNA sequencing. Chemically competent *Escherichia coli* BL21(DE3) cells were transformed with the pDEST17-HisXylS plasmid via heat shock at 42°C using standard protocols. Transformed cells were grown in LB medium supplemented with 100 µg/mL ampicillin at 37°C shaking at 170 rpm, and cell density was monitored by absorbance at 600 nm (A_{600}). Log phase cultures were grown until A_{600} was between 0.4 and 0.6, and protein expression was induced by the addition of isopropyl β-D-1-thiogalactopyranoside (IPTG) to a final concentration of 0.2 mM at 16°C and allowed to incubate for 16 h shaking at 170 rpm. Cells were harvested by centrifugation and stored at −80°C until ready for lysis and purification. Cells were then resuspended in lysis buffer (25 mM HEPES-NaOH pH 7.2, 400 mM NaCl, 20 mM Imidazole,

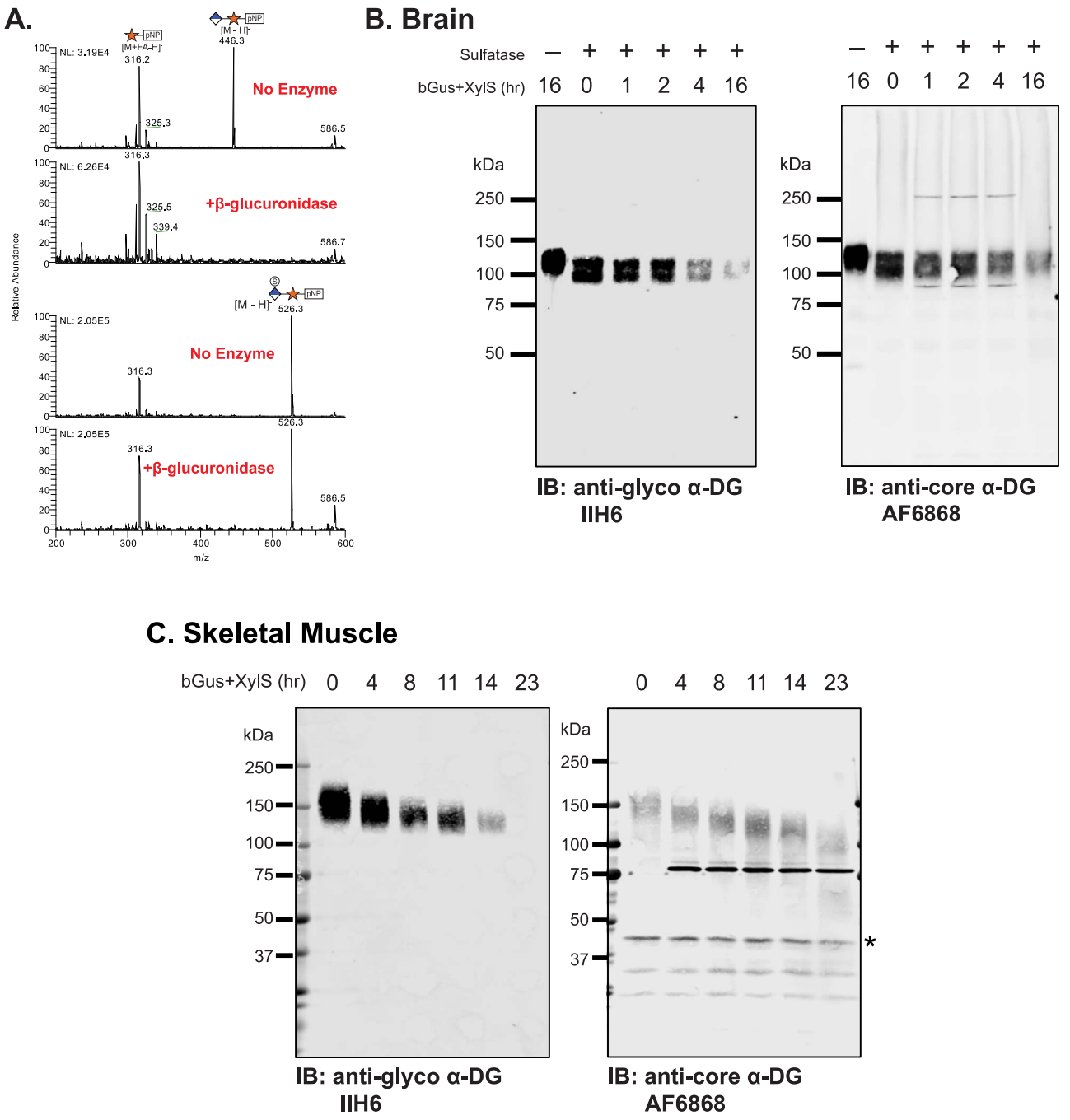

Fig. 5. Sulfation serves as a cap on matriglycan. (A) GlcA-β4-Xyl-β-pNP is amenable to bGus digestion by bGus, while sulfated GlcA-β4-Xyl-β-pNP is not, as detected by ITMS. Spectra shown are representative of $N = 3$. (B) Sulfatase treatment of brain α-DG facilitates dual glycosidase digestion (bGus + XylS) as detected by immunoblot (IB) analysis using the antibody IIH6 that recognizes matriglycan on α-DG, or anti-α-DG-core (AF6868). (C) IIH6 and anti-α-DG-core IBs of exoglycosidase treated skeletal muscle. Asterisk ($*$) indicates β-DG. Results shown are the representative of $N = 3$.

0.3% Triton-X100, 1× Protease Inhibitor Cocktail Set V [EDTA-Free, Millipore Sigma, St. Louis, MO]), probe sonicated for 4 min on ice (cycles of 10 s on and 10 s off), and Pierce™ Universal Nuclease was added to degrade released DNA and RNA to reduce viscosity of the lysate. The lysate was clarified by centrifugation at 17,000 × *g* for 30 min at 4°C, followed by Heat Fractionation by incubation in a 70°C water bath for 10 min. The lysate was again clarified by centrifugation at 17,000 × *g* for 30 min at 4°C. The enzyme (His_6-XylS or simply, XylS) was purified by Ni-NTA chromatography at 4°C, eluted with 300 mM imidazole and buffer exchanged into phosphate buffered saline (PBS), pH 7.2. Protein concentration was determined by bicinchoninic acid assay. The average yield of purified His_6-XylS was 1.6 mg per liter of *E. coli* culture. The enzyme's XylS activity was determined by the hydrolysis of pNP-α-D-Xyl in 100 µL reactions containing various amounts of His_6-XylS in 100 mM NaOAc pH 5.5 at 65°C for 30 min. Assays were quenched

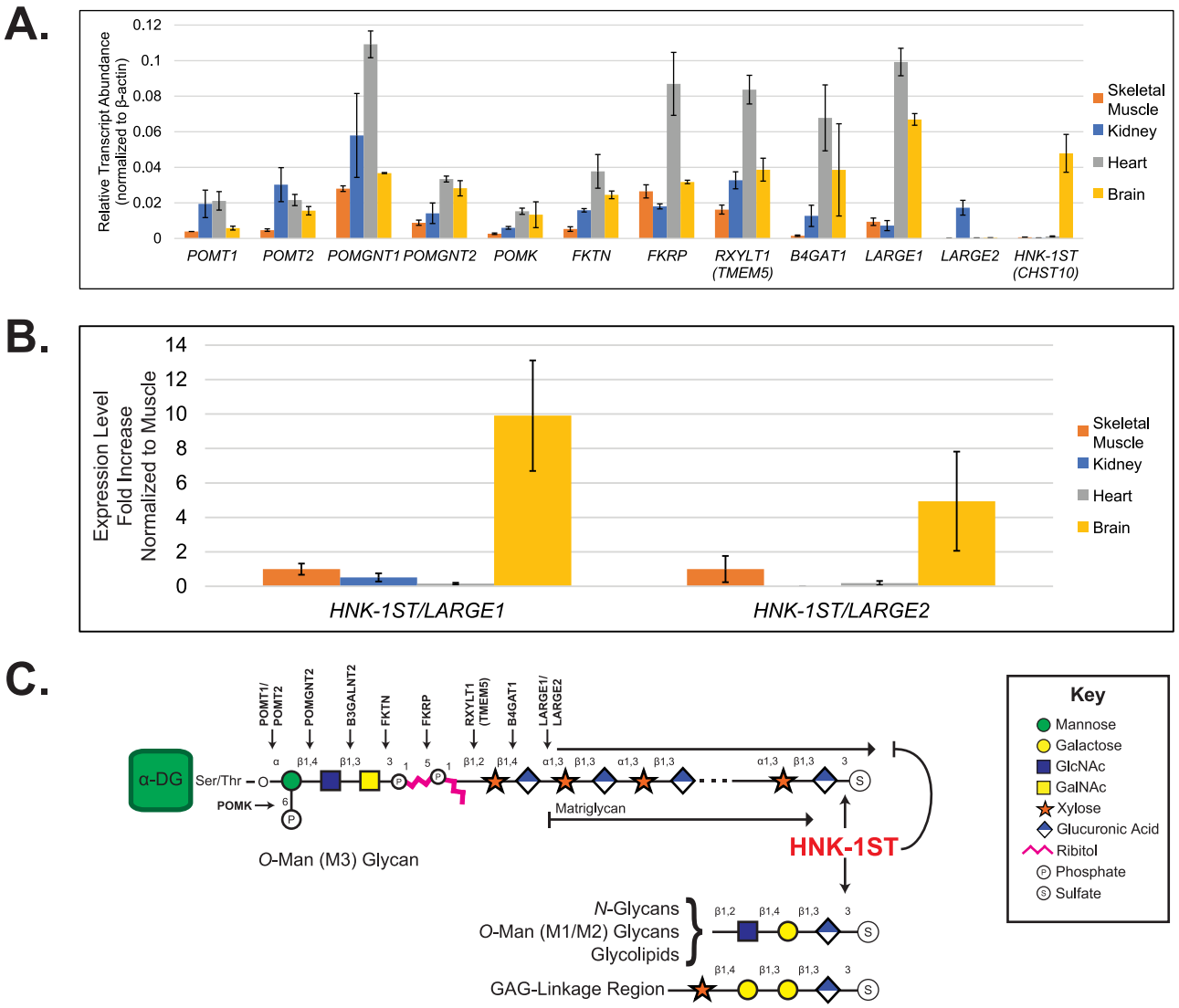

Fig. 6. Transcript analysis of genes involved with Core M3 glycan synthesis. (A) qRT-PCR analysis of transcripts involved with Core M3 glycan synthesis (error bars represent SEM). (B) Comparison of HNK-1ST expression levels from C, relative to LARGE1 or LARGE2, normalized to that of skeletal muscle. (C) Proposed model comparing HNK-1ST activities and effects on matriglycan synthesis. Major enzymes involved with the synthesis of the α-DG Core M3 glycan are indicated. This figure is available in black and white in print and in color at *Glycobiology* online.

by the addition of 100 µL of 50 mM NaOH, and the release of pNP was determined spectrophotometrically by measuring absorbance at 405 nm (A_{405}).

Recombinant expression of soluble, secreted versions of green fluorescent protein (GFP)-B4GAT1 and LARGE1 were expressed and purified as previously described (Praissman et al. 2014). The catalytic domain of human HNK-1ST (Gene symbol CHST10, amino acid residues 28-356, UniProt O43529) (Moremen et al. 2018) was expressed as a soluble, secreted fusion protein (amino-terminal signal sequence, 8 × His-tag, AviTag and 'superfolder' GFP followed by a TEV-protease cleavage site) by transient transfection of HEK293F suspension cultures (Moremen et al. 2018). Suspension culture HEK293F cells (Life Technologies, Grand Island, NY) were transfected as previously described (Meng et al. 2013), and the cell culture media was subjected to Ni-NTA chromatography (Millipore Sigma, St. Louis, MO). Enzyme preparations eluted with 300 mM imidazole were concentrated to ~1 mg/mL using an Amicon centrifugal concentrator (Millipore Sigma) with a 10 kDa molecular weight cutoff and buffer exchanged into PBS pH 7.2.

WGA-enrichment from tissues

Wildtype and Large1$^{myd/myd}$ mouse brain, heart and kidney tissues were dissected and snap frozen in liquid nitrogen. Enrichment of α-DG from these tissues was formed as previously described (Combs and Ervasti 2005; Briggs et al. 2016). Briefly, each tissue sample was minced and homogenized in 50 mM Tris (pH 7.5), 300 mM NaCl, 1% Triton X-100 with protease inhibitors. After clarification by centrifugation, the lysate was applied to WGA agarose beads. The WGA beads were then washed, and bound proteins were eluted with 50 mM Tris (pH 7.5), 300 mM NaCl, 0.1% Triton X-100 and 300 mM GlcNAc. Elution fractions were incubated at 99°C for 5 min in the presence of 10 mM 2-mercaptoethanol, followed by buffer-exchanging into 150 mM sodium acetate pH 5.5, and concentration to a final volume of 200 µL.

Exoglycosidase and sulfatase assays

Exoglycosidase reactions with bGus and XylS were performed as previously described (Briggs et al. 2016). Lyophilized arylsulfatase from *Helix pomatia* (Product #S9626) was purchased from Sigma-Aldrich (St. Louis, MO) and resuspended in 0.2% (w/v) NaCl to a stock concentration of 0.2 units/μL of sulfatase. For each sample, bGus and XylS were added and allowed to incubate at 65°C for 6 h. The pH was neutralized with Tris buffer before loading onto 3–15% polyacrylamide gels for sodium dodecyl sulfate-polyacrylamide gel electrophoresis (SDS-PAGE) and immunoblotting.

For the combined sulfatase/exoglycosidase treatment, α-DG was isolated from the rabbit brain and buffer exchanged into 150 mM sodium acetate pH 5.5 as described above. To ~1 mL of buffer exchanged eluate, 8 units of sulfatase was added and incubated for 24 h at 65°C. Approximately 750 μL of the α-DG sample pretreated with sulfatase was repurified using 100 μL of WGA-agarose beads at 4°C for 1 h, followed by extensive washing with 150 mM sodium acetate pH 5.5 and elution with 150 mM sodium acetate pH 5.5 and 300 mM GlcNAc. The bGus and XylS were added and allowed to incubate at 65°C for 16 h, taking aliquots for analysis at 0, 1, 2, 4 and 16 h. Samples were analyzed by SDS-PAGE and immunoblotting using mAb IIH6 or anticore α-DG (AF6868) as described below. Similarly processed samples from rabbit skeletal muscle were digested with bGus and XylS for 23 h, taking aliquots for analysis at 0, 4, 8, 11, 14 and 23 h.

Immunoblotting and laminin overlay assay

Following SDS-PAGE, proteins were transferred to PVDF-FL (Millipore), and probed with various antibodies as follows: The anti-α-DG core primary antibody (Goat 20 AP, 1:100 dilution; Jung et al. 1996) was detected by secondary antibody donkey anti-goat IgG IR800CW (1:4000, Li-Cor). The anti-glyco α-DG mAb IIH6 (1:100 Dilution, Developmental Studies Hybridoma Bank, University of Iowa; Ervasti and Campbell 1991) was detected by secondary antibody goat anti-mouse IgM IR800CW (1:4000, Li-Cor). Laminin overlay assays were performed as previously described (Michele et al. 2002). Natural mouse laminin from the Engelbreth-Holm-Swarm (EHS) sarcoma was purchased from Invitrogen (23017-015). The rabbit polyclonal anti-laminin antibody (Sigma L9393, 1:1000 dilution) was detected by secondary antibody donkey anti-rabbit IgG IR800CW (1:4000, Li-Cor). All immunoblots were imaged using a Li-Cor Odyssey scanner.

Synthesis of GlcA-β4-Xyl-β-pNP and pNP-matriglycan

The HNK-1ST acceptor substrate, GlcA-β4-Xyl-β-pNP, was generated in a 500 μL reaction containing 16 mM Xyl-β-pNP, 100 mM MOPS pH 7.0, 10 mM $MnCl_2$, 10 mM $MgCl_2$, 20 mM UDP-GlcA, 0.02 U/μL CIAP and 6 μM GFP-B4GAT1. The reaction was allowed to incubate at 37°C for 24 h. Reaction products were purified using C18 MicroSpin Columns (The Nest Group, Southborough, MA) by applying and washing in Buffer A (0.1% formic acid) and elution with Buffer B (0.1% formic acid, 80% acetonitrile). Samples were dried down using a SpeedVac and resuspended in MilliQ water. Aliquots of reaction products, diluted in 50% methanol were analyzed by Direct Infusion into an ITMS (Velos Pro, ThermoFisher Scientific, San Jose, CA) using nanospray ionization in negative ion mode.

pNP-matriglycan was generated in a 300 μL reaction containing 500 μM GlcA-β4-Xyl-β-pNP, 100 mM MES pH 6.0, 10 mM $MnCl_2$, 10 mM $MgCl_2$, 1 mM UDP-GlcA, 1 mM UDP-Xyl, 0.01 U/μL CIAP and 1 μM GFP-LARGE1. The reaction was allowed to incubate at 37°C for 66 h. Reaction products were purified using C18 MicroSpin Columns (The Nest Group) by applying and washing in Buffer A (0.1% formic acid) and elution with Buffer B (0.1% formic acid, 80% acetonitrile). Samples were dried down using a SpeedVac and resuspended in MilliQ water. Aliquots of reaction products, diluted in 50% methanol were analyzed by Direct Infusion into an ITMS (Velos Pro, ThermoFisher Scientific, San Jose, CA) using nanospray ionization in negative ion mode.

HNK-1ST assays

HNK-1ST reactions were performed in 50 mM Tris-HCl pH 7.4, 50 μM GlcA-β4-Xyl-β-pNP (or pNP-matriglycan), 100 μM PAPS (Santa Cruz, Dallas, TX) and 0.2 μM GFP-HNK-1ST. The reaction was allowed to incubate at 37°C for 17 h. Reaction products were purified using C18 MicroSpin Columns (The Nest Group) by applying and washing in Buffer A (0.1% formic acid) and elution with Buffer B (0.1% formic acid, 80% acetonitrile). Samples were dried down using a SpeedVac and resuspended in 50% methanol. Reactions were analyzed by Direct Infusion into an ITMS (Velos Pro, ThermoFisher Scientific, San Jose, CA) using nanospray ionization in negative ion mode. For extension of matriglycan by GFP-LARGE1, After sulfation with HNK-1ST, reaction products were dried down using a SpeedVac and resuspended in a cocktail containing 100 mM MES pH 6.0, 10 mM $MnCl_2$, 10 mM $MgCl_2$, 1 mM UDP-GlcA, 1 mM UDP-Xyl and 1 μM GFP-LARGE1. The reaction was allowed to incubate at 37°C for 16 h. Reaction products were purified using C18 MicroSpin Columns as described above and analyzed by ITMS as described above.

NMR analysis

For NMR analysis, ~0.4 mg of either GlcA-β4-Xyl-β-pNP or SO_3-GlcA-β4-Xyl-β-pNP was prepared as described above. Each sample was resuspended in 99% D_2O (Cambridge Isotope Laboratories, Inc., Tewksbury, MA) and analyzed on an Agilent 900 MHz DD2 spectrometer equipped with a 5-mm cryogenically cooled probe. After stabilization and shimming, NMR experiments were performed at 25°C using standard pulse sequences (PRESAT, gCOSY) from the Agilent library. Two-dimensional data were collected with default values. Spectra were processed with MestReNova software (Mestrelab Research SL). A summary of observed and literature monosaccharide NMR chemical shifts is presented in Table II.

RNA isolation and transcript analysis

Total RNA was isolated from flash frozen skeletal muscle, kidney, heart and brain tissues using the RNeasy kit (Qiagen) following the tissue extraction protocol except that the tissues were homogenized in RLT buffer containing 3% β-mercaptoethanol. Methods for cDNA synthesis and qRT-PCR were described previously (Nairn et al. 2010). Briefly, validated gene specific primer pairs (Table III) were used for technical triplicate reactions with diluted cDNA and iQ™ SYBR® Green Supermix in a RealPlex² Mastercycler (Eppendorf). Relative transcript abundance values for each gene were calculated by normalizing to the housekeeping gene, β-Actin and the SEM from two biological replicates of each tissue were calculated.

Table III. Gene specific primer pairs used in transcript analysis

Gene name	Forward primer (5′–3′)	Reverse primer (5′–3′)	GenBank accession #
POMT1	CTACCTGCCCTTCTTCCTGA	AGCAGGATCTGGAAGGTGAG	NM_145145
POMT2	CTTAAACGGCCTGCTTGGAGC	AAGGACAGCAGCGTCACCAC	NM_153415
POMGNT1	ACAGCTGAGGATCCAGCACT	TTCCTGAGCACCCATCCTAG	NM_026651
POMGNT2	TGACTGAAAGGCTGAACGTG	AGTCTGTTCTGGGTGCGA	NM_001289558
POMK	GGTGGGCTACTGTGAGGAAG	CTTCCAGGTTGCTCAAGGAA	NM_029037
FKTN	AGCTGACCACTCATGCCATCC	CGTAGGTGACCATGCCAGAGG	NM_139309
FKRP	CTAACAACTACCGCCGCTTC	GTACTCCGGGTTCTCGATGA	NM_173430
RXYLT1 (TMEM5)	TTGCTTGGAAATGAGCACTG	CAGATCCACAAAGCCTCCAT	NM_153059
B4GAT1	GGAGAGCTTGCTGAGACCTG	CCTTTCCTCCAGCCACATAA	NM_175383
LARGE1	GCTCACCACCGTGGGAACC	TGCCAGCTCGCAGATTCTCAC	NM_010687
LARGE2	GAGCCTGGCCTTGTACCTGAC	AGAGAGCACTGGCGACGTTTC	NM_172670
HNK-1ST (CHST10)	GATTCGAGCCTTGGTACAGG	GTCCGGTTCTTCCGGTACTT	NM_145142
β-ACTIN	GATCGGTGGCTCCATCCTGG	GCCGGACTCATCGTACTCCTG	NM_007393

Supplementary data

Supplementary Material is available at *GLYCOB* online.

Acknowledgements

We would like to thank all members of the Wells, Campbell and Moremen laboratories for their helpful discussions. The pET-TMGUA-WT plasmid (bGus) was a generous gift from Dr Stephen G. Withers (University of British Columbia). The pT7SCII-XylS plasmid was a generous gift from Dr Marco Moracci (University of Naples Federico II).

Funding

This work was supported in part by grants from NIH/NIGMS (R01GM111939 to LW; P41GM103390, P01GM107012 to KWM, R01GM130915 to KWM and LW), and a Paul D. Wellstone Muscular Dystrophy Cooperative Research Center grant (1U54NS053672 to KPC). KPC is an investigator of the Howard Hughes Medical Institute.

Conflict of interest

KWM is the president and AVN is now an employee of Glyco Expression Technologies, Inc., a biotechnology spinout that focuses on recombinant glycoenzyme production and could conceivably profit from the results described herein.

Abbreviations

B3GAT1, β-1,3-glucuronyltransferase 1 (GlcAT-P); B3GAT2, β-1, 3-glucuronyltransferase 2(GlcAT-S); bGus, *Thermotoga maritima* β-glucuronidase; CMD, congenital muscular dystrophy; COSY, homonuclear correlation spectroscopy; ECM, extracellular matrix; GAG, glycosaminoglycan; GlcA, glucuronic acid; HNK-1ST, HNK-1 sulfotransferase (CHST10); ITMS, ion trap mass spectrometry; LacNAc, *N*-acetyl-D-lactosamine; LARGE1, like-acetylglucosaminyltransferase 1; LARGE2, like-acetylglucosaminyl transferase 2; LG, laminin globular; MAG, myelin-associated glycoprotein; NCAM, neural cell adhesion molecule; PAPS, 3′-phosphoadenosine 5′-phosphosulfate; pNP, *para*-nitrophenyl; UDP, uridine diphosphate; WGA, wheat germ agglutinin; Xyl, xylose; XylS, *sulfolobus solfataricus* α-xylosidase; α-DG, α-dystroglycan

References

Aumailley M, Bruckner-Tuderman L, Carter WG, Deutzmann R, Edgar D, Ekblom P, Engel J, Engvall E, Hohenester E, Jones JC *et al.* 2005. A simplified laminin nomenclature. *Matrix Biol*. 24:326–332.

Bakker H, Friedmann I, Oka S, Kawasaki T, Nifant'ev N, Schachner M, Mantei N. 1997. Expression cloning of a cDNA encoding a sulfotransferase involved in the biosynthesis of the HNK-1 carbohydrate epitope. *J Biol Chem*. 272:29942–29946.

Barresi R, Michele DE, Kanagawa M, Harper HA, Dovico SA, Satz JS, Moore SA, Zhang WL, Schachter H, Dumanski JP *et al.* 2004. LARGE can functionally bypass alpha-dystroglycan glycosylation defects in distinct congenital muscular dystrophies. *Nat Med*. 10:696–703.

Beedle AM, Turner AJ, Saito Y, Lueck JD, Foltz SJ, Fortunato MJ, Nienaber PM, Campbell KP. 2012. Mouse fukutin deletion impairs dystroglycan processing and recapitulates muscular dystrophy. *J Clin Invest*. 122:3330–3342.

Bhunia A, Vivekanandan S, Eckert T, Burg-Roderfeld M, Wechselberger R, Romanuka J, Bachle D, Kornilov AV, von der Lieth CW, Jimenez-Barbero J *et al.* 2010. Why structurally different cyclic peptides can be glycomimetics of the HNK-1 carbohydrate antigen. *J Am Chem Soc*. 132:96–105.

Briggs DC, Yoshida-Moriguchi T, Zheng T, Venzke D, Anderson ME, Strazzulli A, Moracci M, Yu L, Hohenester E, Campbell KP. 2016. Structural basis of laminin binding to the LARGE glycans on dystroglycan. *Nat Chem Biol*. 12:810–814.

Brockington M, Torelli S, Sharp PS, Liu K, Cirak S, Brown SC, Wells DJ, Muntoni F. 2010. Transgenic overexpression of LARGE induces alpha-dystroglycan hyperglycosylation in skeletal and cardiac muscle. *PLoS One*. 5:e14434.

Chou DK, Ilyas AA, Evans JE, Costello C, Quarles RH, Jungalwala FB. 1986. Structure of sulfated glucuronyl glycolipids in the nervous system reacting with HNK-1 antibody and some IgM paraproteins in neuropathy. *J Biol Chem*. 261:11717–11725.

Combs AC, Ervasti JM. 2005. Enhanced laminin binding by alpha-dystroglycan after enzymatic deglycosylation. *Biochem J*. 390: 303–309.

Dwyer CA, Katoh T, Tiemeyer M, Matthews RT. 2015. Neurons and glia modify receptor protein-tyrosine phosphatase zeta (RPTPzeta)/phosphacan with cell-specific O-mannosyl glycans in the developing brain. *J Biol Chem*. 290:10256–10273.

Ervasti JM, Campbell KP. 1991. Membrane organization of the dystrophin-glycoprotein complex. *Cell*. 66:1121–1131.

Ervasti JM, Campbell KP. 1993. A role for the dystrophin-glycoprotein complex as a transmembrane linker between laminin and actin. *J Cell Biol*. 122:809–823.

Gerin I, Ury B, Breloy I, Bouchet-Seraphin C, Bolsee J, Halbout M, Graff J, Vertommen D, Muccioli GG, Seta N *et al.* 2016. ISPD produces CDP-

ribitol used by FKTN and FKRP to transfer ribitol phosphate onto alpha-dystroglycan. *Nat Commun*. 7:11534.

Grewal PK, Holzfeind PJ, Bittner RE, Hewitt JE. 2001. Mutant glycosyltransferase and altered glycosylation of alpha-dystroglycan in the myodystrophy mouse. *Nat Genet*. 28:151–154.

Grewal PK, McLaughlan JM, Moore CJ, Browning CA, Hewitt JE. 2005. Characterization of the LARGE family of putative glycosyltransferases associated with dystroglycanopathies. *Glycobiology*. 15:912–923.

Hall H, Deutzmann R, Timpl R, Vaughan L, Schmitz B, Schachner M. 1997. HNK-1 carbohydrate-mediated cell adhesion to laminin-1 is different from heparin-mediated and sulfatide-mediated cell adhesion. *Eur J Biochem*. 246:233–242.

Hall H, Liu L, Schachner M, Schmitz B. 1993. The L2/Hnk-1 carbohydrate mediates adhesion of neural cells to laminin. *Eur J Neurosci*. 5: 34–42.

Hashiguchi T, Mizumoto S, Nishimura Y, Tamura J, Yamada S, Sugahara K. 2011. Involvement of human natural killer-1 (HNK-1) sulfotransferase in the biosynthesis of the GlcUA(3-O-sulfate)-gal-gal-Xyl tetrasaccharide found in alpha-thrombomodulin from human urine. *J Biol Chem*. 286:33003–33011.

Hohenester E. 2018. Laminin G-like domains: Dystroglycan-specific lectins. *Curr Opin Struct Biol*. 56:56–63.

Inamori K, Hara Y, Willer T, Anderson ME, Zhu Z, Yoshida-Moriguchi T, Campbell KP. 2013. Xylosyl- and glucuronyltransferase functions of LARGE in alpha-dystroglycan modification are conserved in LARGE2. *Glycobiology*. 23:295–302.

Inamori K, Yoshida-Moriguchi T, Hara Y, Anderson ME, Yu L, Campbell KP. 2012. Dystroglycan function requires xylosyl- and glucuronyltransferase activities of LARGE. *Science*. 335:93–96.

Jung D, Duclos F, Apostol B, Straub V, Lee JC, Allamand V, Venzke DP, Sunada Y, Moomaw CR, Leveille CJ *et al.* 1996. Characterization of delta-sarcoglycan, a novel component of the oligomeric sarcoglycan complex involved in limb-girdle muscular dystrophy. *J Biol Chem*. 271:32321–32329.

Kanagawa M, Kobayashi K, Tajiri M, Manya H, Kuga A, Yamaguchi Y, Akasaka-Manya K, Furukawa J, Mizuno M, Kawakami H *et al.* 2016. Identification of a post-translational modification with ribitol-phosphate and its defect in muscular dystrophy. *Cell Rep*. 14:2209–2223.

Kanagawa M, Toda T. 2018. Ribitol-phosphate-a newly identified posttranslational glycosylation unit in mammals: Structure, modification enzymes and relationship to human diseases. *J Biochem*. 163:359–369.

Kizuka Y, Oka S. 2012. Regulated expression and neural functions of human natural killer-1 (HNK-1) carbohydrate. *Cell Mol Life Sci*. 69:4135–4147.

Kleene R, Schachner M. 2004. Glycans and neural cell interactions. *Nat Rev Neurosci*. 5:195–208.

Kruse J, Mailhammer R, Wernecke H, Faissner A, Sommer I, Goridis C, Schachner M. 1984. Neural cell adhesion molecules and myelin-associated glycoprotein share a common carbohydrate moiety recognized by monoclonal antibodies L2 and HNK-1. *Nature*. 311:153–155.

Kunz S, Rojek JM, Kanagawa M, Spiropoulou CF, Barresi R, Campbell KP, Oldstone MB. 2005. Posttranslational modification of α-dystroglycan, the cellular receptor for arenaviruses, by the glycosyltransferase LARGE is critical for virus binding. *J Virol*. 79:14282–14296.

Manya H, Endo T. 2017. Glycosylation with ribitol-phosphate in mammals: New insights into the O-mannosyl glycan. *Biochim Biophys Acta Gen Subj*. 1861:2462–2472.

Manya H, Yamaguchi Y, Kanagawa M, Kobayashi K, Tajiri M, Akasaka-Manya K, Kawakami H, Mizuno M, Wada Y, Toda T *et al.* 2016. The muscular dystrophy gene TMEM5 encodes a ribitol beta1,4-xylosyltransferase required for the functional glycosylation of dystroglycan. *J Biol Chem*. 291:24618–24627.

McDearmon EL, Combs AC, Sekiguchi K, Fujiwara H, Ervasti JM. 2006. Brain alpha-dystroglycan displays unique glycoepitopes and preferential binding to laminin-10/11. *FEBS Lett*. 580:3381–3385.

McGarry RC, Helfand SL, Quarles RH, Roder JC. 1983. Recognition of myelin-associated glycoprotein by the monoclonal antibody HNK-1. *Nature*. 306:376–378.

Meng L, Forouhar F, Thieker D, Gao Z, Ramiah A, Moniz H, Xiang Y, Seetharaman J, Milaninia S, Su M *et al.* 2013. Enzymatic basis for N-glycan sialylation: Structure of rat alpha2,6-sialyltransferase (ST6GAL1) reveals conserved and unique features for glycan sialylation. *J Biol Chem*. 288:34680–34698.

Michele DE, Barresi R, Kanagawa M, Saito F, Cohn RD, Satz JS, Dollar J, Nishino I, Kelley RI, Somer H *et al.* 2002. Post-translational disruption of dystroglycan-ligand interactions in congenital muscular dystrophies. *Nature*. 418:417–422.

Moracci M, Cobucci Ponzano B, Trincone A, Fusco S, De Rosa M, van Der Oost J, Sensen CW, Charlebois RL, Rossi M. 2000. Identification and molecular characterization of the first alpha-xylosidase from an archaeon. *J Biol Chem*. 275:22082–22089.

Moremen KW, Ramiah A, Stuart M, Steel J, Meng L, Forouhar F, Moniz HA, Gahlay G, Gao Z, Chapla D *et al.* 2018. Expression system for structural and functional studies of human glycosylation enzymes. *Nat Chem Biol*. 14:156–162.

Morise J, Kizuka Y, Yabuno K, Tonoyama Y, Hashii N, Kawasaki N, Manya H, Miyagoe-Suzuki Y, Takeda S, Endo T *et al.* 2014. Structural and biochemical characterization of O-mannose-linked human natural killer-1 glycan expressed on phosphacan in developing mouse brains. *Glycobiology*. 24:314–324.

Morise J, Takematsu H, Oka S. 2017. The role of human natural killer-1 (HNK-1) carbohydrate in neuronal plasticity and disease. *Biochim Biophys Acta Gen Subj*. 1861:2455–2461.

Nairn AV, dela Rosa M, Moremen KW. 2010. Transcript analysis of stem cells. *Methods Enzymol*. 479:73–91.

Nakagawa N, Izumikawa T, Kitagawa H, Oka S. 2011. Sulfation of glucuronic acid in the linkage tetrasaccharide by HNK-1 sulfotransferase is an inhibitory signal for the expression of a chondroitin sulfate chain on thrombomodulin. *Biochem Biophys Res Commun*. 415:109–113.

Nakagawa N, Manya H, Toda T, Endo T, Oka S. 2012. Human natural killer-1 sulfotransferase (HNK-1ST)-induced sulfate transfer regulates laminin-binding glycans on alpha-dystroglycan. *J Biol Chem*. 287:30823–30832.

Nakagawa N, Takematsu H, Oka S. 2013. HNK-1 sulfotransferase-dependent sulfation regulating laminin-binding glycans occurs in the post-phosphoryl moiety on alpha-dystroglycan. *Glycobiology*. 23:1066–1074.

Ong E, Suzuki M, Belot F, Yeh JC, Franceschini I, Angata K, Hindsgaul O, Fukuda M. 2002. Biosynthesis of HNK-1 glycans on O-linked oligosaccharides attached to the neural cell adhesion molecule (NCAM): The requirement for core 2 beta 1,6-N-acetylglucosaminyltransferase and the muscle-specific domain in NCAM. *J Biol Chem*. 277:18182–18190.

Patnaik SK, Stanley P. 2005. Mouse large can modify complex N- and mucin O-glycans on alpha-dystroglycan to induce laminin binding. *J Biol Chem*. 280:20851–20859.

Peyrard M, Seroussi E, Sandberg-Nordqvist AC, Xie YG, Han FY, Fransson I, Collins J, Dunham I, Kost-Alimova M, Imreh S *et al.* 1999. The human LARGE gene from 22q12.3-q13.1 is a new, distinct member of the glycosyltransferase gene family. *Proc Natl Acad Sci U S A*. 96:598–603.

Praissman JL, Live DH, Wang S, Ramiah A, Chinoy ZS, Boons GJ, Moremen KW, Wells L. 2014. B4GAT1 is the priming enzyme for the LARGE-dependent functional glycosylation of alpha-dystroglycan. *Elife*. 3.

Praissman JL, Wells L. 2014. Mammalian O-mannosylation pathway: Glycan structures, enzymes, and protein substrates. *Biochemistry-Us*. 53:3066–3078.

Praissman JL, Willer T, Sheikh MO, Toi A, Chitayat D, Lin YY, Lee H, Stalnaker SH, Wang S, Prabhakar PK *et al.* 2016. The functional O-mannose glycan on α-dystroglycan contains a phospho-ribitol primed for matriglycan addition. *Elife*. 3:03943.

Riemersma M, Froese DS, van Tol W, Engelke Udo F, Kopec J, van Scherpenzeel M, Ashikov A, Krojer T, von Delft F, Tessari M *et al.* 2015. Human ISPD is a cytidyltransferase required for dystroglycan O-mannosylation. *Chem Biol*. 22:1643–1652.

Roscioli T, Kamsteeg EJ, Buysse K, Maystadt I, van Reeuwijk J, van den Elzen C, van Beusekom E, Riemersma M, Pfundt R, Vissers LE *et al.* 2012. Mutations in ISPD cause Walker-Warburg syndrome and defective glycosylation of alpha-dystroglycan. *Nat Genet*. 44:581–585.

Salleh HM, Mullegger J, Reid SP, Chan WY, Hwang J, Warren RA, Withers SG. 2006. Cloning and characterization of *Thermotoga maritima* beta-glucuronidase. *Carbohydr Res*. 341:49–59.

Sheikh MO, Halmo SM, Wells L. 2017. Recent advancements in understanding mammalian O-mannosylation. *Glycobiology*. 27:806–819.

Smirnov SP, McDearmon EL, Li SH, Ervasti JM, Tryggvason K, Yurchenco PD. 2002. Contributions of the LG modules and furin processing to laminin-2 functions. *J Biol Chem*. 277:18928–18937.

Suzuki-Anekoji M, Suzuki A, Wu SW, Angata K, Murai KK, Sugihara K, Akama TO, Khoo KH, Nakayama J, Fukuda MN *et al.* 2013. In vivo regulation of steroid hormones by the Chst10 sulfotransferase in mouse. *J Biol Chem*. 288:5007–5016.

Talts JF, Andac Z, Gohring W, Brancaccio A, Timpl R. 1999. Binding of the G domains of laminin alpha 1 and alpha 2 chains and perlecan to heparin, sulfatides, alpha-dystroglycan and several extracellular matrix proteins. *EMBO J*. 18:863–870.

Tisi D, Talts JF, Timpl R, Hohenester E. 2000. Structure of the C-terminal laminin G-like domain pair of the laminin alpha 2 chain harbouring binding sites for alpha-dystroglycan and heparin. *EMBO J*. 19:1432–1440.

Varki A, Cummings RD, Aebi M, Packer NH, Seeberger PH, Esko JD, Stanley P, Hart G, Darvill A, Kinoshita T *et al.* 2015. Symbol nomenclature for graphical representations of Glycans. *Glycobiology*. 25:1323–1324.

Voshol H, van Zuylen CW, Orberger G, Vliegenthart JF, Schachner M. 1996. Structure of the HNK-1 carbohydrate epitope on bovine peripheral myelin glycoprotein P0. *J Biol Chem*. 271:22957–22960.

Wells L. 2013. The o-mannosylation pathway: Glycosyltransferases and proteins implicated in congenital muscular dystrophy. *J Biol Chem*. 288:6930–6935.

Willer T, Inamori K, Venzke D, Harvey C, Morgensen G, Hara Y, Beltran Valero de Bernabe D, Yu L, Wright KM, Campbell KP. 2014. The glucuronyltransferase B4GAT1 is required for initiation of LARGE-mediated alpha-dystroglycan functional glycosylation. *Elife*. 3:03941.

Willer T, Lee H, Lommel M, Yoshida-Moriguchi T, de Bernabe DB, Venzke D, Cirak S, Schachter H, Vajsar J, Voit T *et al.* 2012. ISPD loss-of-function mutations disrupt dystroglycan O-mannosylation and cause Walker-Warburg syndrome. *Nat Genet*. 44:575–580.

Xiao ZC, Bartsch U, Margolis RK, Rougon G, Montag D, Schachner M. 1997. Isolation of a tenascin-R binding protein from mouse brain membranes. A phosphacan-related chondroitin sulfate proteoglycan. *J Biol Chem*. 272:32092–32101.

Yagi H, Yanagisawa M, Suzuki Y, Nakatani Y, Ariga T, Kato K, Yu RK. 2010. HNK-1 epitope-carrying tenascin-C spliced variant regulates the proliferation of mouse embryonic neural stem cells. *J Biol Chem*. 285:37293–37301.

Yoshida-Moriguchi T, Campbell KP. 2015. Matriglycan: A novel polysaccharide that links dystroglycan to the basement membrane. *Glycobiology*. 25:702–713.

Yoshida-Moriguchi T, Willer T, Anderson ME, Venzke D, Whyte T, Muntoni F, Lee H, Nelson SF, Yu LP, Campbell KP. 2013. SGK196 is a glycosylation-specific O-mannose kinase required for dystroglycan function. *Science*. 341:896–899.

Yoshida-Moriguchi T, Yu LP, Stalnaker SH, Davis S, Kunz S, Madson M, Oldstone MBA, Schachter H, Wells L, Campbell KP. 2010. O-mannosyl phosphorylation of alpha-dystroglycan is required for laminin binding. *Science*. 327:88–92.

Yuen CT, Chai W, Loveless RW, Lawson AM, Margolis RU, Feizi T. 1997. Brain contains HNK-1 immunoreactive O-glycans of the sulfoglucuronyl lactosamine series that terminate in 2-linked or 2,6-linked hexose (mannose). *J Biol Chem*. 272:8924–8931.